# Fe-amino acid complexes, immobilised on silica gel as active and highly selective catalysts in cyclohexene epoxidation

**Gábor Varga · Zita Csendes · Éva G. Bajnóczi · Stefan Carlson · Pál Sipos · István Pálinkó✉**

**Abstract** In this work the syntheses, structure, superoxide dismutase (SOD) activity and the catalytic use in the oxidative transformations of cyclohexene of covalently grafted Fe(III)–complexes formed with various or various combinations of C-protected amino acid (L-histidine, L-tyrosine, L-cysteine and L-cystine) ligands is presented. The structural features of the surface complexes were studied by XANES/EXAFS and mid/far IR spectroscopies. The compositions of the complexes were determined by ICP-MS and the Kjeldahl method. The superoxide dismutase activities of the materials were evaluated in a biochemical test reaction. The obtained materials were used as catalysts for the oxidation of cyclohexene with peracetic acid in acetone. Both covalent grafting and building the complex onto the surface of the chloropropylated silica gel were successful in all cases. In many instances the obtained structures and the coordinating groups were found to substantially vary upon changing the conditions of the syntheses. All the covalently immobilised Fe(III)–complexes displayed more or less superoxide dismutase activity and were found to be capable of catalysing the oxidation of cyclohexene with high activities and outstanding epoxide selectivities.

**Keywords**: silica-anchored · Fe(III)−C-protected amino acids · covalent anchoring · structural characterisation · catalytic activity and selectivity

G. Varga · Z. Csendes · I. Pálinkó ✉
Department of Organic Chemistry, University of Szeged,
Dóm tér 8, Szeged, H-6720 Hungary
e-mail: palinko@chem.u-szeged.hu

É.G. Bajnóczi · P. Sipos
Department of Inorganic and Analytical Chemistry, University of Szeged,
Dóm tér 7, Szeged, H-6720 Hungary

G. Varga · Z. Csendes · É.G. Bajnóczi · O. Berkesi · P. Sipos · I. Pálinkó
Material and Solution Structure Research Group, Institute of Chemistry, University of Szeged,
Dóm tér 7-8 Szeged, H-6720 Hungary

S. Carlson
MaxIV-Lab, Lund University,
SE-223 63 Lund, Sweden Lund, Sweden

## Introduction

Enzymes catalyse a wide-range of chemical transformations. They often provide high regio- and stereoselectivity and operate under physiological conditions. Enzyme-catalysed reactions can be alternatives to traditional organic syntheses under environmentally benign conditions [1]. Outside the usual physiological environment, such as extreme temperature, pH or presence of non-aqueous solvents, enzymes are unstable and are easily inactivated. Therefore, they have several limitations for broader applications, like catalysts in the synthesis of fine chemicals. Moreover, the recovery and the reuse of enzymes are also cumbersome. These drawbacks can be eliminated and more stable and reusable catalysts may be produced by immobilising the enzyme over various supports by employing methods that preserve the catalytic activity and selectivity of the support-free enzyme [2, 3].

Active and selective solid catalysts can also be fabricated by immobilising either the active site itself, or its structural or functional model. [4]. Both approaches are applied in various laboratories, and promising results emerge. These biomimetic catalysts comprise of redox-active transition metal ions, [5] complexed by amino acids [6] or other molecules that are capable of coordination [7]. The immobilised complexes are often called bioinspired catalysts and their activities and selectivities may resemble to those of the enzymes. These substances are capable of being operational under more rigorous conditions and they can easily be recovered and recycled [8].

In this contribution, the active centre of the Fe(III) superoxide dismutase (SOD) enzyme was used for inspiration. Superoxide dismutase enzymes protect cells from the attack of superoxide radical anions. These radical species are generated in small quantities during $O_2$ metabolism and responsible for inflammation, neuronal degeneration, diabetes, cancer and ageing. Nature has evolved four different SOD enzymes (Cu,ZnSOD [9], NiSOD [10], MnSOD [11] and FeSOD [12]) that convert these reactive species to oxygen and hydrogen peroxide through a dismutation reaction. The Fe- and the MnSOD enzymes are homologous both in their structure and amino acid sequence and considered to form a single class of SOD enzymes [13]. They are dimers or tetramers with one Mn or Fe ion per monomer unit and with a molecular weight of 22 kDa. The geometry around the metal ion is trigonal bipyramidal, coordinated by two histidine and one aspartate ligands in the equatorial plane and a histidine and a solvent molecule in the axial plane. The solvent molecule, that is $OH^-$ in

the oxidised and $H_2O$ in the reduced form of the enzyme, is supported by an extensive network of H-bonds [14, 15].

There is hope to obtain efficient, durable and recoverable electron transfer catalysts that can be reused, if one can immobilise the functional mimics of this enzyme in a way or another (*e.g.*, hydrogen bonding, ion-exchange, covalent anchoring) on solid supports of various kinds (*e.g.*, zeolites, layered materials, resins, unmodified or surface-modified silica gel).

This hope is supported by a range of literature results. Some of them are briefly described in the followings.

Fe(III)–Schiff base complexes, immobilised in zeolite Y, were active and selective in the oxidation of cyclooctane and no metal leaching was observed during the reaction [16]. Anionic Fe(III) porphyrins, intercalated into ZnAl-LDHs and were successfully used in alkene oxidations [17].

Covalent binding is a strong, primary bond between the enzyme or the metal complex and the support; therefore, the catalysts do not suffer from leaching during the catalytic reactions. The main disadvantages of this type of anchoring are that the support is usually unusable after the deactivation of the catalyst resulting in additional costs and the enzyme conformation may change upon anchoring, leading to decrease in enzyme activity. Nevertheless, this is the most widely used method for immobilisation. Mostly polymers and silicates are used as supports, since choosing suitable reagents, reactive functional groups can be easily created on their surface [18−20].

A short peptide, with His-Glu-Glu-Glu motif was immobilised on silica carrier *via* solid-phase peptide synthesis, and their Cu(II) and Fe(III) complexes were constructed *via* self-assembly. The catalysts displayed excellent catalytic activities in the oxidation of cyclohexane, and there was no metal leaching detected [21].

Catalytic epoxidation of alkenes by various oxidants is of interest since epoxides are intermediates and precursors to many useful chemical products [22], such as food additives, agrochemicals, drugs, [23] perfumes and sweeteners [24]. Cyclohexene oxide is used in the synthesis of many products, *e.g.*, chiral pharmaceuticals, epoxy paints, pesticides, dyestuffs and rubber promoters [25].

Mainly hydrogen peroxide, organic peroxides (*tert*-butyl hydroperoxide), peracids (peracetic acid, *m*-chloroperbenzoic acid) and molecular oxygen are used as oxidants for oxidation of alkenes [26].

$H_2O_2$ is an attractive primary oxidant for liquid-phase reactions, since it is relatively cheap, readily available and useful for the synthesis of fine chemicals [27].

*tert*-Butyl hydroperoxide (TBHP) is also a suitable oxygen source, since it can be easily activated by transition metal complexes, has good thermal stability and is soluble in non-polar solvents [28].

Peracids can epoxidise alkenes without adding catalyst; however, for the uncatalysed reaction relatively high reaction temperatures and long reaction times are needed [29]. These drawbacks can be eliminated by adding transition metal catalyst to the reaction [30]. Molecular oxygen or even air is the cheapest, the most environmentally benign and readily available oxidant, many researchers try to activate it with biomimetic catalysts [31].

In the followings, a summary is given based on previously published results [32, 33] on the construction, structural characterisation and SOD-like activity testing of Fe(III)−C-protected uniform or mixed amino acid complexes covalently anchored chloropropylated silica gel, inspired by the active centre of the FeSOD enzyme, and an account is provided on these features of newly constructed silica-anchored complexes. Furthermore, the hitherto unpublished results concerning the catalytic activities and selectivities of all these anchored complexes are also communicated here.

## Experimental

### Materials and methods of syntheses

For the syntheses, C-protected (in the form of methyl ester) L-histidine, L-tyrosine, L-cysteine and L-cystine were used as ligands. The metal ion source was $FeCl_3 \cdot 6H_2O$. Chloropropylated silica gel (SG − particle size: 230–400 mesh, BET surface area: 500 $m^2/g$, functionalisation: 8%)] was used as support. These materials as well as the 2-propanol solvent were products of Aldrich Chemical Co. All the chemicals were of analytical grade and were used without further purification.

The general features of the syntheses are as follows. The first step of immobilisation was the reaction of the appropriately protected amino acid (1.75 mmol) and the support (0.5 g, containing 0.35 mmol of chlorine atoms). The C-protected amino acids were covalently grafted onto the support through N-alkylation like reaction by

refluxing the mixture in 2-propanol (60 $cm^3$) under alkaline conditions. After 24 h, the solid substance was filtered, washed several times in order to remove the uncoupled amino acid excess and dried. Complexation followed the anchoring: the grafted support was soaked in the 2-propanolic (60 $cm^3$) solution of the metal salt (1.75 mmol) under continuous stirring at room temperature for 24 h. After filtering and washing, the obtained material was divided into two parts. Half of it was set aside. This is what we call *covalent grafting under ligand-poor conditions*, *i.e.*, only the immobilised protected amino acids were available for coordination. To the other half, 2-propanolic (60 $cm^3$) solution of the appropriately protected amino acid derivative was added in excess (0.875 mmol), and the suspension was continuously stirred at room temperature for 24 h. Then, the solid material was filtered, rinsed with 2-propanol several times and dried. Latter was named *covalent grafting under ligand-excess conditions*, *i.e.*, the surface-grafted complex might have rearranged in the presence of excess amino acid mixture.

Surface-grafted complexes were prepared having both uniform and mixed amino acid derivatives (two protected amino acids were used) as ligands. Two methods were applied for the syntheses when mixed ligands were used. In method '*A'*, one of the protected amino acid ester was covalently anchored to the surface of the support; then, it was soaked in the metal salt solution, and after filtering and thorough washing the final substance was made by allowing complexation with excess amounts of the other amino acid ester. In method '*B'* a 1:1 molar mixture of the protected amino acids was grafted onto the surface of the support; then, the metal complex was formed. Parts of the materials thus formed were further treated in excess 1:1 protected amino acid mixtures resulting in the formation of surface-anchored complexes under ligand-excess conditions. The other experimental parameters were the same as described above.

The materials used for catalytic testing in the electron transfer reactions of cyclohexene and their codes used in the followings are listed as follows:

SG–His-OMe–Fe(III)[a] complex made under ligand-poor conditions,

SG–His-OMe–Fe(III)–H-His-OMe[a] complex made under ligand-excess conditions,

SG–Tyr-OMe–Fe(III)[a],

SG–Cys-OMe–Fe(III),

SG–Cys-OMe–Fe(III)–H-Cys-OMe,

SG–$(Cys\text{-}OMe)_2$–Fe(III),

SG–$(Cys\text{-}OMe)_2$–Fe(III)M–H-$(Cys\text{-}OMe)_2$,

SG–His-OMe–Fe(III)–H-Tyr-OMe[a],

SG–Tyr-OMe–Fe(III)–H-His-OMe[a],

SG–His-OMe;Tyr-OMe–Fe(III)[a],

SG–His-OMe;Tyr-OMe–Fe(III)–H-His-OMe;H-Tyr-OMe[a],

SG–His-OMe–Fe(III)–H-Cys-OMe[b],

SG–Cys-OMe–Fe(III)–H-His-OMe[b],

SG–His-OMe;Cys-OMe–Fe(III)[b],

SG–His-OMe;Cys-OMe–Fe(III)–H-His-OMe;H-Cys-OMe[a],

SG–His-OMe–Fe(III)–$(H\text{-}Cys\text{-}OMe)_2$,

SG–$(Cys\text{-}OMe)_2$–Fe(III)–H-His-OMe,

SG–His-OMe;$(Cys\text{-}OMe)_2$–Fe(III),

SG–His-OMe;$(Cys\text{-}OMe)_2$–Fe(III)–H-His-OMe;$(H\text{-}Cys\text{-}OMe)_2$.

a, b – synthesis, structural characterisation and SOD-like activity is described in refs. [32] and [33], respectively.

## Analytical measurements

The amount of Fe(III) ions on the surface-modified silica gel was measured by an Agilent 7700x ICP−MS. Before measurements, a few milligrams of the anchored complexes measured by analytical accuracy were digested in 1 $cm^3$ cc. $H_2SO_4$; then, they were diluted with distilled water to 50 $cm^3$ and filtered.

The nitrogen content of the samples was determined by the Kjeldahl method. 5 $cm^3$ cc. $H_2SO_4$ and 1 $cm^3$ 30% solution of $H_2O_2$ were added to approximately 100 mg of the grafted complexes weighed by analytical accuracy. $CuSO_4 \cdot 5H_2O$ was used as catalyst to increase the boiling point of the medium. The reaction mixture was boiled for some hours, to obtain colourless mixture from the initially dark-coloured suspension. Then it was diluted with 40 $cm^3$ distilled water and was distilled with a 20% solution of sodium hydroxide in the presence of phenolphthalein indicator. The released ammonia was absorbed in 0.1 M solution of HCl. Then, the remainder acid was titrated with 0.1 M solution of NaOH in the presence of methyl orange indicator.

## X-ray absorption spectroscopy (XAS) measurements

The major characteristics of this method are described briefly in the followings. XAS is the measurement of the X-ray absorption coefficient of a material as a function of energy. X-ray energies are high enough to eject one or more core electrons from an atom, *via* the photoelectric effect. These electrons have well-defined binding energies. The absorption coefficient decreases with the increase in energy, until it reaches the binding energy of an inner electron. This is the absorption edge of the element. At this point a sharp peak appears in the spectrum and the corresponding energy is the so-called threshold energy.

The importance of XAS derives from the fact that there is fine structure superimposed on the absorption edge. This fine structure is often divided into X-ray absorption near edge structure (XANES), for structure in the immediate vicinity of the edge and extended X-ray absorption fine structure (EXAFS), referring to structure well above the absorption edge. The various regions of the X-ray absorption spectrum provide different information. XANES gives information on the bonding character, the oxidation state and the coordination geometry of the element studied, while from the EXAFS region structural parameters like coordination number, bond lengths, *etc.* can be extracted.

The measurements were carried out on the K-edge of the metals at MAX-lab at beamline I811. This is a superconducting multipole wiggler beamline equipped with a water-cooled channel cut Si(111) double crystal monochromator delivering at 10 keV, approximately $2\times10^{15}$ photons/s/0.1% bandwidth with horizontal and vertical FWHM of 7 and 0.3 mrad, respectively [34]. A beamsize of 0.5 mm × 1.0 mm (width × height) was used. The incident beam intensity ($I_0$) was measured with an ionisation chamber filled with a mixture of $He/N_2$. Higher order harmonics were reduced by detuning the second monochromator to 50−70% of the maximum intensity, depending on the metal. Data collection was performed in transmission mode. ~300 mg samples were measured in Teflon spacers with Kapton tape windows. Data were treated by the Demeter program package [35, 36].

XAS spectra were normalised to an edge jump of unity and the background absorption was removed.

The EXAFS data were $k^3$-weighted and Fourier transformed in the range of $k$ = 2−12 $Å^{-1}$. The ranges for the backtransform were 1–3 Å for all complexes. The fitted parameters included the amplitude reduction factor ($S_0^2$), interatomic distances (R), Debye-Waller factors ($\sigma^2$) and energy shift ($\Delta E_0$). The coordination numbers (N) were

kept constant during each optimisation, but a range of coordination numbers were used to find the best fit.

The main objectives of these measurements were to determine the coordination numbers, geometries around the Fe(III) ion, and to find out whether the sulphur atom was coordinated to the central ion in the anchored Fe(III) complexes.

Mid/far range FT-IR spectroscopy

Structural information on each step of the synthesis procedure was obtained by far- and mid-range infrared spectroscopy. Mid-range spectra were recorded with a BIO-RAD Digilab Division FTS-65 A/896 FT-IR spectrophotometer with 4 $cm^{-1}$ resolution, measuring diffuse reflectance. 256 scans were collected for each spectrum. 300 mg KBr and 10 mg sample were combined and finely grounded. Spectra were evaluated by the Win-IR package. They were baseline-corrected, smoothed (if it was necessary) and the spectra of the supports were subtracted. The 3800–600 $cm^{-1}$ wavenumber range was investigated. The comparison of the difference mid IR spectra of the anchored amino acid derivatives with and without metal ion, and the spectra of the pristine amino acid derivatives gives indirect information on the coordinating groups. The difference $\Delta$ [$\Delta = \nu_{asym(COO-)} - \nu_{sym(COO-)}$] between the asymmetric and symmetric carboxylate vibrations gives information about the coordination mode of the carboxylate group. The coordination can be either bidentate chelating ($\Delta_{complex} < \Delta_{ligand}$) or bidentate bridging ($\Delta_{complex} \sim \Delta_{ligand}$) or monodentate ($\Delta_{complex} > \Delta_{ligand}$) [37]. A shift in the position of the carbonyl group and the phenolic C–O or the absence of the S–H stretching vibration indicates the participation of these groups in complexation [38, 39].

Far-range spectra were recorded with a BIO-RAD Digilab Division FTS-40 vacuum FT-IR spectrophotometer with 4 $cm^{-1}$ resolution. 256 scans were collected for each spectrum. The Nujol mull technique was used between two polyethylene windows (the suspension of 10 mg sample and a drop of Nujol mull). Spectra were evaluated by the Win-IR package. They were baseline-corrected and smoothed (if it was necessary). Unfortunately, in several cases the spectra could not be used for evaluation. The spectra in the far IR region provide direct information on metal ion–functional group coordination, although assignation of the vibrations in the far IR spectra is not a trivial exercise. For making it easier probe complexes having uniform, thus easily identifiable

coordinating groups were prepared and their far IR spectra were registered. Fe(III) complexes of imidazole, isopropylamine and monosodium malonate were prepared. Each probe complex was synthesised *via* using 2-propanol (10 $cm^3$) as solvent. The metal salt ($4\times10^{-4}$ mol) and the ligand ($2.4\times10^{-3}$ mol) were stirred for 24 h at room temperature to get solid precipitate. The obtained materials were filtered and washed with 2-propanol.

Testing the superoxide dismutase activity

The SOD activity was tested by the Beauchamp-Fridovich reaction [40]. A brief description of this biochemical test reaction is as follows. For this reaction riboflavin, L-methionine and nitro blue tetrazolium were used. Under aerobic conditions reaction takes place on illumination between riboflavin and L-methionine. It is a reduction and the reduced form of riboflavin reacts with oxygen forming a peroxide derivative. This derivative decomposes giving the superoxide radical anion. This radical ion is captured by the nitro blue tetrazolium (NBT) and its original yellow colour turns blue.

The transformation can be followed by Vis spectrophotometry, measuring the absorbance at 560 nm. If our enzyme mimicking material works well, it successfully competes with NBT in capturing the superoxide radical ion. Thus, the photoreduction of NBT is inhibited. The SOD probe reaction was carried out at room temperature in a suspension of the immobilised complex at pH = 7 ensured with a phosphate or for the Mn(II) complexes, 4-(2-hydroxyethyl)-1-piperazineethanesulfonic acid (HEPES) buffer. The reaction mixture contained 0.1 $cm^3$ of 0.2 mM riboflavin, 0.1 $cm^3$ of 5 mM NBT, 2.8 $cm^3$ of 50 mM buffer, containing EDTA (0.1 mM), L-methionine (13 mM) and the catalyst. Riboflavin was added last and the reaction was initiated by illuminating the tubes with two 15 W fluorescent lamps. Equilibrium could be reached in 10 minutes. EDTA masks the interfering metal ion traces, since the metal ion–EDTA complexes have no SOD activity. From the resulting graph the volume of enzyme mimicking complex corresponding to 50% inhibition ($IC_{50}$) was registered to allow a comparison with the efficiency of the real enzyme and other SOD mimics. The enzyme mimic works the better when the $IC_{50}$ is the smaller. There was no reaction without illumination and the support did not display SOD activity either.

Catalytic oxidation of cyclohexene

In the reaction a vial with septum was loaded with the catalyst (25 mg), acetone (10 ml), cyclohexene (5 mmol) and 2.5 mmol peracetic acid (~39% in acetic acid). After 3 h of continuous stirring at room temperature, the mixture was analysed quantitatively by a Hewlett-Packard 5890 Series II gas chromatograph (GC) using an Agilent HP-1 column and the internal standard technique. The temperature was increased in stages from 50 ºC to 250 ºC. The products were identified *via* the use of authentic samples.

## Results and discussion

Analytical measurements

The results of the Kjeldahl method and the ICP–MS measurements for the grafted Fe(III)–complexes containing uniform ligands are displayed in Table 1.

In all cases, the metal ion to amino acid ratios indicate (they are never integers) that mixtures of various kinds of complexes were formed on the surface. The amino acid content of SG–Tyr-OMe–Fe(III) and SG–Tyr-OMe–Fe(III)–H-Tyr-OMe is almost the same, suggesting that the preparation of the complex under ligand-excess conditions was not successful. For the SG–His-OMe–Fe(III)–H-His-OMe complex the ratio was 5.8 indicating either six-fold coordination, or rather that H-HisOMe tends to adsorb over the silica gel surface firmly, and even extraction with 2-propanol for two days could not remove it.

**Table 1** Amino acid and $Fe^{3+}$ content of the samples obtained from Kjeldahl type N-determination and ICP-MS measurements

| Sample | Amino acid content (mmol/g) | $Fe^{3+}$ content (mmol/g) |
|---|---|---|
| SG–His-OMe–Fe(III) | 0.596 | 0.497 |
| SG–His-OMe–Fe(III)–H-His-OMe | 2.897 | 0.496 |
| SG–Tyr-OMe–Fe(III) | 0.572 | 0.380 |
| SG–Tyr-OMe–Fe(III)–H-Tyr-OMe | 0.581 | 0.382 |
| SG–Cys-OMe–Fe(III) | 0.460 | 0.333 |
| SG–Cys-OMe–Fe(III)–H-Cys-OMe | 0.654 | 0.333 |
| SG–$(Cys\text{-}OMe)_2$–Fe(III) | 0.445 | 0.370 |
| SG–$(Cys\text{-}OMe)_2$–Fe(III)–H-$(Cys\text{-}OMe)_2$ | 0.924 | 0.371 |

X-ray absorption measurements

Fe K-edge XAS spectra were recorded for some complexes formed with sulphur-containing ligands. The XANES spectra of the materials are depicted in Fig. 1.

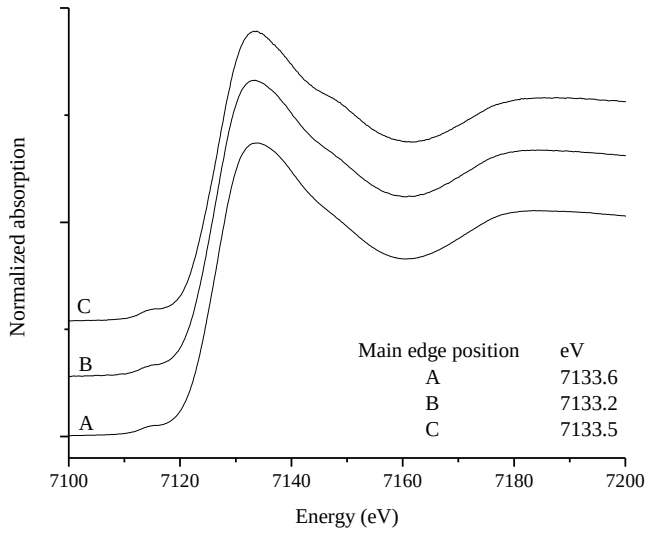


**Fig. 1** The Fe K-edge XANES spectra of A – SG–$(Cys\text{-}OMe)_2$–Fe(III), B – SG–Cys-OMe–Fe(III), C – SG–His-OMe–Fe(III)–H-Cys-OMe

Since the local symmetry around the Fe is higher in octahedral than in tetrahedral complexes, the intensity of the characteristic pre-edge peak around 7113 eV decreases in the following order: $I_{tetrahedral} > I_{square\ pyramidal} > I_{octahedral}$ [41].

Comparison of the normalised intensity of the pre-edge peak in the anchored Fe(III) complexes (I ~ 0.05) with that of some reference compounds indicates that the complexes are 5-coordinate; they are square pyramidal [42].

The Fourier-transformed EXAFS data (without phase correction) are displayed in Fig. 2, and the results of the fitting are shown in Table 2.

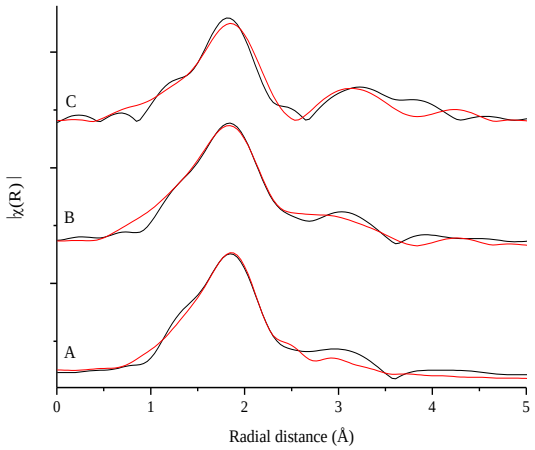


**Fig. 2** The Fourier-transformed EXAFS data (without phase correction) of A – SG–$(Cys\text{-}OMe)_2$–Fe(III), B – SG–Cys-OMe–Fe(III), C – SG–His-OMe–Fe(III)–H-Cys-OMe, red line – fit, black line – experimental

**Table 2** Parameters deduced from the fitted EXAFS spectra (N – coordination number, R – bond length, $\sigma^2$ – Debye-Waller factor, $\Delta E_0$ – energy shift, R factor – goodness of fit).

| Sample | $(Fe^{3+}–)X$ | N | R (Å) | $\sigma^2$ (Å$^2$) | $\Delta E_0$ (eV) | R factor |
|---|---|---|---|---|---|---|
| SG–$(Cys\text{-}OMe)_2$–Fe(III) | O/N | 5 | 1.98 | 0.0080 | -1.44 | 0.0179 |
| SG–Cys-OMe–Fe(III) | O/N | 4 | 1.98 | 0.0120 | -5.37 | 0.0135 |
| | S | 1 | 2.36 | 0.0327 | | |
| SG–His-OMe–Fe(III)–H-Cys-OMe | O/N | 3.6 | 1.98 | 0.0114 | -5.69 | 0.0120 |
| | S | 1.4 | 2.36 | 0.0232 | | |

In the first coordination shell of SG–$(Cys\text{-}OMe)_2$–Fe(III), there are five oxygen/nitrogen atoms, with a Fe(III)–O/N bond length of 1.98 Å. For SG–Cys-OMe–Fe(III), the first coordination sphere contains four O/N atoms and one sulphur atom,

where the bond distances were fitted to be 1.98 and 2.36 Å, respectively. In SG–His-OMe–Fe(III)–H-Cys-OMe, the Fe(III)–O/N distance is 1.98 Å and the average coordination number is 3.6, while for Fe(III)–S these date are 2.36 Å and 1.4, respectively. The thiolate sulphur donor atom is coordinated to the Fe(III) irrespective to whether the cysteine is anchored or non-anchored on the surface of the support.

Mid/far range FT-IR spectroscopy

In Fig. 3 (trace A), the difference spectrum of SG–His-OMe–Fe(III) is displayed. The $\nu_{asym(COO-)}$ and $\nu_{sym(COO-)}$ stretching frequencies of the anchored complex are observed at 1630 $cm^{-1}$ and 1399 $cm^{-1}$, respectively. $\Delta$ = 231 $cm^{-1}$, for the ligand it is 170 $cm^{-1}$. This difference confirms the monodentate nature of the coordinated carboxylate group. The difference spectrum of SG–His-OMe–Fe(III) can be seen in the far IR range in Figure 4, spectrum A. The band at 256 $cm^{-1}$ indicates that one of the imidazole nitrogen takes part in the complexation. The bands at 352 and 326 $cm^{-1}$ may be assigned to the Fe(III)–$O_{carboxylate}$ bond. Bidentate binding is quite conceivable under ligand-poor conditions, since there is not enough surface-anchored amino acids in close vicinity to each other for monodentate coordination.

Regarding the mid IR difference spectrum of SG–His-OMe–Fe(III)–H-His-OMe (Fig. 3, trace B) it is clear that the surface-anchored complex prepared under ligand-poor conditions rearranged in the presence of excess C-protected histidine. The position of the carbonyl band (1751 $cm^{-1}$) changed relative to that of the free histidine methylester (1761 $cm^{-1}$), indicating the coordination of the carbonyl oxygen. The Fe(III)–$N_{imidazole}$ stretching vibration is observed at 265 $cm^{-1}$ (Fig. 4, trace B). The bands above 400 $cm^{-1}$ can be assigned as coordinated water/ligand vibrations.

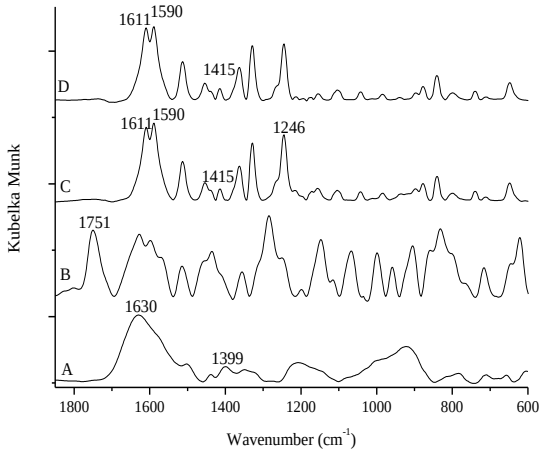


**Fig. 3** The difference IR spectra of A – SG–His-OMe–Fe(III), B – SG–His-OMe–Fe(III)–H-His-OMe, C – SG–Tyr-OMe–Fe(III), D – SG–Tyr-OMe–Fe(III)–H-Tyr-OMe (the spectrum of the support was subtracted)

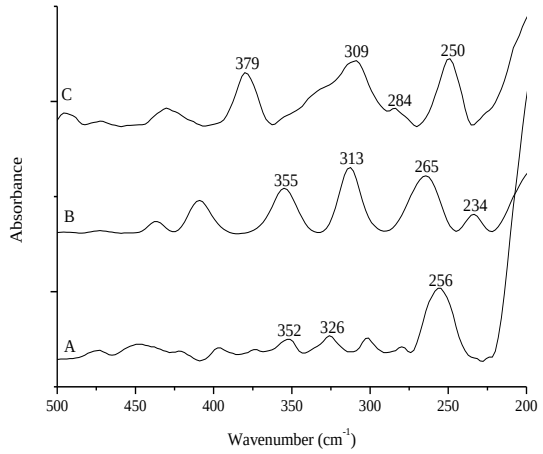


**Figure 4** The difference far IR spectra of A – SG–His-OMe–Fe(III), B – SG–His-OMe–Fe(III)–H-His-OMe, C – SG–Tyr-OMe–Fe(III) (the spectrum of the support was subtracted)

For SG–Tyr-OMe–Fe(III), $\Delta$ = 1611 $cm^{-1}$ – 1415 $cm^{-1}$ = 196 $cm^{-1}$ indicating monodentate coordination of the carboxylate group, since for the ligand this difference is 151 $cm^{-1}$ (Fig. 3, trace C). The phenolate oxygen is coordinated to the central ion, since the phenolate C–$O^{-}$ vibration of the anchored ligand is observed at 1280 $cm^{-1}$ shifted1246 $cm^{-1}$ in the surface-anchored complex. It is easy to observe that the spectra SG–Tyr-OMe–Fe(III) and SG–Tyr-OMe–Fe(III)–H-Tyr-OMe (Fig. 3, trace D) are the same. This means that ligand-excess condition did not result the rearrangement of the surface complex, as it was expected from the results provided by the Kjeldahl method.

In the far IR range (Fig. 4, trace C), the bands at 379 and 284 $cm^{-1}$ reveal that the nitrogen of the secondary amine, which is formed upon covalent grafting, is a coordinating group.

On the basis of the above-listed results and chemical considerations, the following structures for the covalently immobilised complexes may be proposed:

SG–His-OMe–Fe(III)[a']

$N_{imidazoleHissurf}O_{carboxylateHissurf}H_2O,H_2O,H_2O,$

SG–His-OMe–Fe(III)–H-His-OMe[a]

$N_{imidazoleHissurf}O_{carboxylateHissurf}O_{carbonylHis}N_{imidazoleHis}H_2O,$

SG–Tyr-OMe–Fe(III)[a']

$O_{carboxylateTyrsurf}O_{phenolateTyrsurf},N_{amineTyrsurf}H_2O,H_2O,$

a – coordination sphere proposed in ref. [32],

a' – modified proposal relative to that published in ref. [32] based on new measurements (Kjeldahl, XAS and far IR).

As far as SG–Cys-OMe–Fe(III) is concerned (Fig. 5, trace A), the carboxylate group is most probably coordinated as monodentate ligand, since Δ increased from 190 to 216 $cm^{-1}$ (1602 $cm^{-1}$ – 1386 $cm^{-1}$). The XAS measurement revealed the coordination of the thiolate sulphur, and the lack of the S–H vibration further confirms that. Under ligand-excess conditions (Fig. 5, trace B) the carbonyl oxygen is not involved in the coordination, since the stretching vibration of the carbonyl band did not shift to lower wavenumbers (1745 $cm^{-1}$). There is no S−H vibration at around 2500 $cm^{-1}$; therefore, the thiolate sulphur is coordinated.

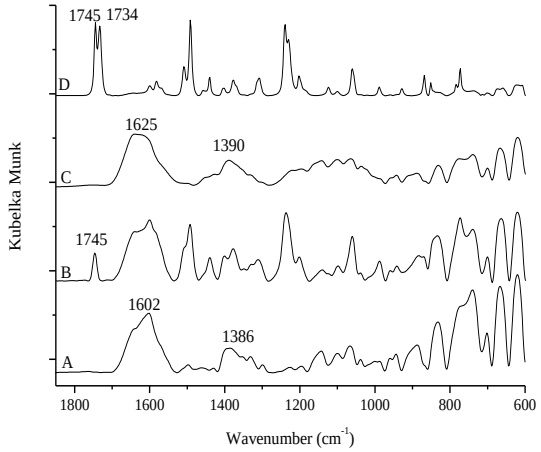


**Fig. 5** The difference IR spectra of A – SG–Cys-OMe–Fe(III), B – SG–Cys-OMe–Fe(III)–H-Cys-OMe, C – $SG–(Cys\text{-}OMe)_2–Fe(III)$,

D – SG–(Cys-OMe)$_2$–Fe(III)–(H-Cys-OMe)$_2$ (the spectrum of the support was subtracted)

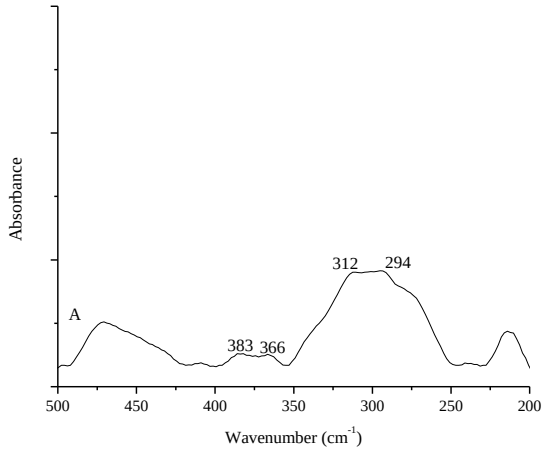


**Fig. 6** The difference far IR spectra of A– SG–(Cys-OMe)$_2$–Fe(III)–(H-Cys-OMe)$_2$ (the spectrum of the support was subtracted)

For the SG–(Cys-OMe)$_2$–Fe(III), $\Delta$ =1625 cm$^{-1}$ – 1390 cm$^{-1}$ = 235 cm$^{-1}$ suggesting the monodentate ligation of the carboxylate groups (Figure 5, trace C). Under ligand-excess conditions (Fig. 5, trace D), the carbonyl oxygens do not take part in the complexation, since the positions of the bands (1745, 1734 cm$^{-1}$) do not move relative to the pristine amino acid. In the far IR range (Fig. 6, trace A) the bands at 383 and 294 cm$^{-1}$ correspond to the Fe(III)–$N_{amino}$ vibrations.

Using all these pieces of information structural proposals for the surface-bound complexes are offered as follows:

SG–Cys-OMe–Fe(III)

$S_{thiolateCyssurf}O_{carboxylateCysssurf}H_2O,H_2O,H_2O,$

SG–Cys-OMe–Fe(III)–H-Cys-OMe

$S_{thiolateCyssurf}O_{carboxylateCysssurf}S_{thiolateCys}S_{thiolateCys}H_2O,$

SG–(Cys-OMe)$_2$–Fe(III)

$O_{carboxylate(Cys)2surf}O_{carboxylate(Cys)2surf}H_2O,H_2O,H_2O,$

SG–(Cys-OMe)$_2$–Fe(III)–(H-Cys-OMe)$_2$

$O_{carboxylate(Cys)2surf}O_{carboxylate(Cys)2surf}N_{amino(Cys)2}N_{amino(Cys)2}H_2O.$

Fig. 7, trace A depicts the difference spectrum of SG–His-OMe–Fe(III)–H-Tyr-OMe. The structure of SG–His-OMe–Fe(III) was determined above. It is clear that the addition of C-protected tyrosine rearranged the surface complex. The stretching

vibration of the carbonyl band shifted to 1687 $cm^{-1}$ from 1745 $cm^{-1}$, indicating that the carbonyl oxygen appeared in the coordination sphere of the metal ion.

For SG–(Tyr-OMe)–Fe(III)–(H-His-OMe) (Fig. 7, trace B), the carbonyl oxygen of C-protected histidine took part in the complexation, since the position of the carbonyl band, which was found to be at 1761 $cm^{-1}$ in the spectrum of the free histidine methylester, moved to 1743 $cm^{-1}$.

Studying the mid IR difference spectra of SG–(His-OMe,Tyr-OMe)–Fe(III) (Fig. 7, trace C), reveals that the carboxylate vibrations of amino acids cannot be separated, but one may assume that the coordination modes of the amino acid are the same as in the complexes with uniform amino acids as ligands.

As far as the spectrum of the anchored complex prepared under ligand-excess conditions is concerned (Fig. 7, trace D), similarity with spectrum of the neat C-protected histidine can be observed: the carbonyl band did not shift. There are no characteristic peaks of C-protected tyrosine, indicating that from the added 1:1 molar mixture of the amino acids only the histidine methylester takes part in the complexation *via* the imidazole nitrogen.

The above-detailed observations may be concluded in the following coordination environments:

SG–His-OMe–Fe(III)–H-Tyr-OMe[a]

$N_{imidazoleHissurf}O_{carboxylateHissurf}O_{carbonylTyr}N_{aminoTyr}H_2O$,

SG–Tyr-OMe–Fe(III)–H-His-OMe[a']

$O_{carboxylateTyrsurf}N_{amineTyrsurf}O_{phenolateTyrsurf}N_{imidazoleHis}O_{carbonylHis}$,

SG–His-OMe;Tyr-OMe–Fe(III)[a']

$N_{imidazoleHissurf}O_{carboxylateHissurf}N_{amineTyrsurf}O_{phenolateTyrsurf}O_{carboxylateTyrsurf}$,

SG–His-OMe;Tyr-OMe–Fe(III)–H-His-OMe;H-Tyr-OMe[a']

$N_{imidazoleHissurf}O_{carboxylateHissurf}O_{carboxylateTyrsurf}O_{phenolateTyrsurf}N_{imidazoleHis}$.

a – coordination sphere proposed in ref. [32],

a' – modified proposal relative to that published in ref. [32] based on a more elaborate interpretation of the IR spectra.

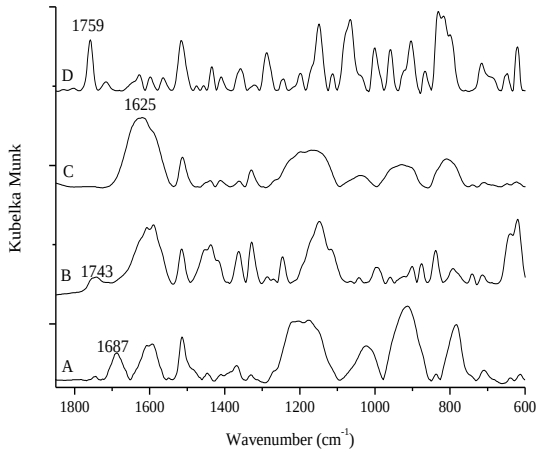


**Fig. 7** The difference IR spectra of A – SG–His-OMe–Fe(III)–H-Tyr-OMe, B – SG–Tyr-OMe–Fe(III)–H-His-OMe, C – SG–His-OMe;Tyr-OMe–Fe(III), D – SG–His-OMe;Tyr-OMe–Fe(III)–H-His-OMe;H-Tyr-OMe (the spectrum of the support was subtracted)

The spectrum of SG–His-OMe–Fe(III)–H-Cys-OMe (Fig. 8, trace A) is very similar to that of the pristine cysteine methylester, while spectrum B resembles that of the unanchored histidine methylester (SG–Cys-OMe–Fe(III)–H-His-OMe). This means that the added amino acid ester rearranged the complex formed upon soaking the silica gel, containing the covalently bonded (other) amino acid in the Fe(III) salt solution. Analysis of the spectra reveals that the carbonyl oxygen of the added C-protected amino is not coordinated, since the position of the carbonyl band hardly changed relative to that of the free amino acid methylester. The absence of the S–H vibration confirms that the thiolate sulphur participates in the complexation, as it was learnt from EXAFS measurements.

As far as SG–His-OMe;Cys-OMe–Fe(III) is concerned (Fig. 8, trace C), the amino acids are proposed to coordinate the same way, when they were used separately, since their vibrations cannot be separated. Spectrum D indicates that histidine methylester is only coordinated from the 1:1 H-His-OMe, H-Cys-OMe mixture added in excess. It can also be learnt that its carbonyl oxygen is not a coordinating site, since its position did not shift on adding the mixture to the material prepared under ligand-poor conditions.

The proposed coordination modes are the followings:

SG–His-OMe–Fe(III)–H-Cys-OMe[a']

$N_{imidazoleHissurf}O_{carboxylateHissurf}S_{thiolateCys}S_{thiolateCys}H_2O$,

SG–Cys-OMe–Fe(III)–H-His-OMe[a']

$S_{thiolateCyssurf}O_{carboxylateCysssurf}N_{imidazoleHis}N_{imidazoleHis}H_2O$,

SG–His-OMe;Cys-OMe–Fe(III)[a']

$N_{imidazoleHissurf}O_{carboxylateHissurf}S_{thiolateCyssurf}O_{carboxylateCysssurf}H_2O$,

SG–His-OMe;Cys-OMe–Fe(III)–H-His-OMe;H-Cys-OMe[a']

$N_{imidazoleHissurf}O_{carboxylateHissurf}S_{thiolateCyssurf}O_{carboxylateCysssurf}N_{imidazoleHis}$.

a' – modified proposal relative to that published in ref. [33] based on a more elaborate interpretation of the IR spectra.

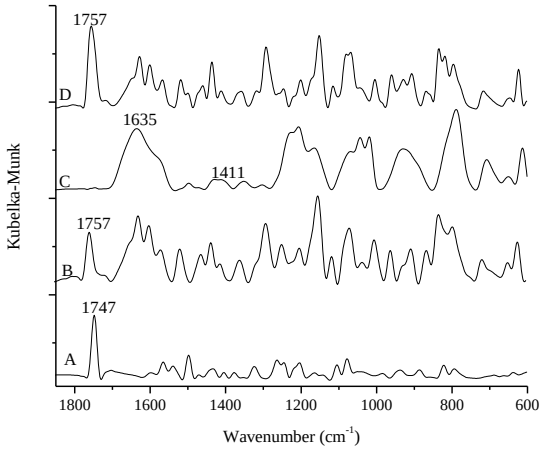


**Fig. 8** The difference IR spectra of A – SG–His-OMe–Fe(III)–H-Cys-OMe, B – SG–Cys-OMe–Fe(III)–H-His-OMe, C – SG–His-OMe;Cys-OMe–Fe(III), D – SG–His-OMe;Cys-OMe–Fe(III)–H-His-OMe;H-Cys-OMe (the spectrum of the support was subtracted)

SG–His-OMe–Fe(III) was rearranged by adding C-protected cystine in excess (Fig. 9, trace A). The stretching vibration of the carbonyl bands (1739 $cm^{-1}$) did not move relative to the free C-protected cysteine; therefore, it can only coordinate with the amino nitrogens.

In Fig. 9, trace B depicts the spectrum of SG–$(Cys\text{-}OMe)_2$–Fe(III)–H-His-OMe. The spectrum is very similar to that of the C-protected histidine − the carbonyl oxygen does not participate in the complexation.

In SG–His-OMe;$(Cys\text{-}OMe)_2$–Fe(III), the anchored amino acids are again assumed to coordinate as they did alone. (Fig. 9, trace C).

Under ligand-excess conditions (Fig. 9, trace D), three unshifted carbonyl vibrations can be seen at 1760 (C-protected histidine), 1746 and 1734 $cm^{-1}$ (C-protected cystine). Unfortunately, their far IR spectra are unusable, but on the basis of these

observations and the accumulated knowledge described at the complexes formed with uniform ligands, the following structures may be proposed:

SG–His-OMe–Fe(III)–$(H\text{-}Cys\text{-}OMe)_2$

$N_{imidazoleHissurf}O_{carboxylateHissurf}N_{amino(Cys)2}N_{amino(Cys)2}H_2O$,

SG–$(Cys\text{-}OMe)_2$–Fe(III)–H-His-OMe

$O_{carboxylate(Cys)2surf}O_{carboxylate(Cys)2surf}N_{imidazoleHis}N_{imidazoleHis}H_2O$,

SG–His-OMe;$(Cys\text{-}OMe)_2$–Fe(III)

$N_{imidazoleHissurf}O_{carboxylateHissurf}O_{carboxylate(Cys)2surf}O_{carboxylate(Cys)2surf}H_2O$,

SG–His-OMe;$(Cys\text{-}OMe)_2$–Fe(III)–H-His-OMe;$(H\text{-}Cys\text{-}OMe)_2$

$N_{imidazoleHissurf}O_{carboxylateHissurf}O_{carboxylate(Cys)2surf}N_{imidazoleHis}N_{amino(Cys)2}$.

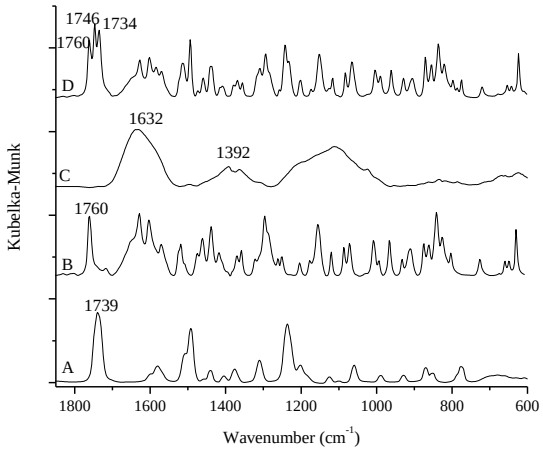


**Fig. 9** The difference IR spectra of A – SG–His-OMe–Fe(III)–$(H\text{-}Cys\text{-}OMe)_2$, B – SG–$(Cys\text{-}OMe)_2$–Fe(III)–H-His-OMe, C – SG–His-OMe;$(Cys\text{-}OMe)_2$–Fe(III), D – SG–His-OMe;$(Cys\text{-}OMe)_2$–Fe(III)–H-His-OMe;$(H\text{-}Cys\text{-}OMe)_2$ (the spectrum of the support was subtracted)

Superoxide dismutase activity of the complexes

All materials were active in catalysing the dismutation reaction of the superoxide radical anion. Catalytic activities differed widely though (Table 3).

Data reveal that there were catalysts with activity close to that of the Cu,ZnSOD enzyme. The most active substances contain cysteine indicating the key role of cysteine-like structures in determining catalytic activity. They seem to have the optimum structures for promoting this reaction. SG–Tyr-OMe–Fe(III) was the second most active

material, in which tyrosine coordinates as tridentate ligand, making the complex more strained.

**Table 3** The SOD activities of the surface grafted complexes

| Materials | $IC_{50}$ (μM) |
|---|---|
| Cu,ZnSOD enzyme | 0.4 |
| SG–His-OMe–Fe(III)a | 57 |
| SG–His-OMe–Fe(III)–H-His-OMea | 47 |
| SG–Tyr-OMe–Fe(III)a | 5 |
| SG–Cys-OMe–Fe(III) | 6 |
| SG–Cys-OMe–Fe(III)–H-Cys-OMe | 31 |
| SG–$(Cys\text{-}OMe)_2$–Fe(III) | 36 |
| SG–$(Cys\text{-}OMe)_2$–Fe(III)–H-$(Cys\text{-}OMe)_2$ | 33 |
| SG–His-OMe–M–Fe(III)-Tyr-OMe[a] | 132 |
| SG–Tyr-OMe–Fe(III)–H-His-OMe[a] | 30 |
| SG–His-OMe;Tyr-OMe–Fe(III)[a] | 34 |
| SG–His-OMe;Tyr-OMe–Fe(III)–H-His-OMe;H-Tyr-OMe[a] | 78 |
| SG–His-OMe–Fe(III)–H-Cys-OMe[b] | 28 |
| SG–Cys-OMe–Fe(III)–H-His-OMe[b] | 25 |
| SG–His-OMe;Cys-OMe–Fe(III)[b] | 21 |
| SG–His-OMe;Cys-OMe–Fe(III)–H-His-OMe;H-Cys-OMe[b] | 4 |
| SG–His-OMe–Fe(III)–$(H\text{-}Cys\text{-}OMe)_2$ | 24 |
| SG–$(Cys\text{-}OMe)_2$–Fe(III)–H-His-OMe | 32 |
| SG–His-OMe;$(Cys\text{-}OMe)_2$–Fe(III) | 31 |
| SG–His-OMe;$(Cys\text{-}OMe)_2$–Fe(III)–H-His-OMe;$(H\text{-}Cys\text{-}OMe)_2$ | 28 |

a, b – data published in refs. [32] and [33], respectively, are shown for comparison

Catalytic oxidation of cyclohexene

The catalytic oxidation of cyclohexene takes place according to Scheme 1 [41]:

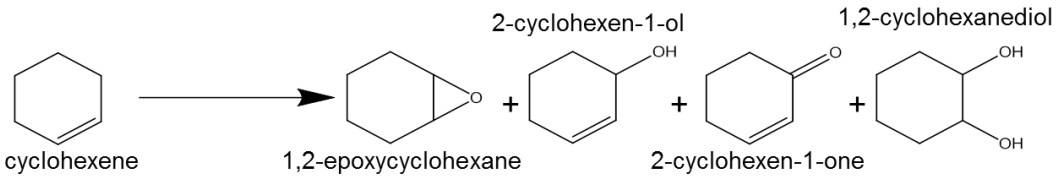


**Scheme 1** The oxidative transformations of cyclohexene

In this reaction, non-heme iron(III) catalyst supported on silica resulted in 2-cyclohexen-1-ol and 2-cyclohexen-1-one as the main products in $CH_3CN$ using $H_2O_2$. The reaction time was 24 h., and the catalyst could be reused with a yield loss of ~4% per use [42]. Maximum 18% conversion of cyclohexene could be reached by iron(III)-salen intercalated in α-zirconium phosphate, in the presence of TBHP after 6 h, when the substrate:oxidant ratio was 5. The major oxidation product was 2-cyclohexen-1-one (75%) [43].

After performing numerous optimisation experiments, we found that for our supported Fe(III) complexes 3 h reaction time and 2.5 mmol peracetic acid were needed to obtain the highest epoxide selectivity, and the reactions must have been performed in acetone to avoid the decomposition of the oxidant. As the activity and selectivity data in Table 4 attest that all the chosen immobilised complexes were catalytically active, and that the major product of the reactions was the epoxide. It is to be seen that in many cases the conversion of catalysed reaction was significantly higher than that of the stoichiometric, even though the catalytic activity were dependent on the amino acid ligands. However, selectivities, which were very significantly higher for the catalysed reaction than for the stoichiometric one, virtually did not depend on the identity of the amino acid ligand. The presence of the ligands were necessary though, since silica gel impregnated with the Fe(III) ions only decomposed the peracetic acid.

As concerns epoxide selectivity and catalytic activity, the best catalsyst is SG–Cys-OMe–Fe(III)–H-Cys-OMe with 99% and 56% conversion, respectively. In general, cysteine-containing materials did not catalyse this reaction well (but the epoxide selectivities are still high), moreover, for SG–$(Cys\text{-}OMe)_2$–Fe(III)–H-$(Cys\text{-}OMe)_2$ the observed conversion was lower than that of the homogeneous, uncatalysed reaction. Significant leaching of the catalyst was not observed, and the catalysts, highlighted in red in Table 4, could be reused twice.

**Table 4** The conversion and selectivity results of the oxidation of cyclohexene after 3 h; the best catalysts are highlighted in red

| Catalyst | Conversion (%) | Epoxide (%) | Alcohol (%) | Ketone (%) | Diol (%) |
|---|---|---|---|---|---|
| – | 21 | 64 | 4 | 2 | 30 |
| SG–His-OMe–Fe(III) | 47 | 89 | 1 | 3 | 7 |
| SG–Tyr-OMe–Fe(III) | 45 | 94 | 2 | 1 | 3 |
| SG–Cys-OMe–Fe(III) | 59 | 87 | 3 | 8 | 2 |
| SG–Cys-OMe–Fe(III)–H-Cys-OMe | 56 | 99 | 1 | 0 | 0 |
| SG–$(Cys\text{-}OMe)_2$–Fe(III) | 25 | 97 | 1 | 1 | 1 |
| SG–$(Cys\text{-}OMe)_2$–Fe(III)–H-$(Cys\text{-}OMe)_2$ | 10 | 95 | 2 | 1 | 2 |
| SG–His-OMe–Fe(III)–H-Cys-OMe | 44 | 88 | 2 | 0 | 10 |
| SG–Cys-OMe–Fe(III)–H-His-OMe | 65 | 85 | 2 | 9 | 4 |
| SG–His-OMe;Cys-OMe–Fe(III) | 49 | 98 | 1 | 0 | 1 |
| SG–His-OMe;Cys-OMe–Fe(III)–H-His-OMe;H-Cys-OMe | 32 | 97 | 1 | 1 | 1 |

The mechanism of the reaction is suggested as follows: one of the coordinated water molecule is replaced by the peroxidic oxygen donor oxidant, forming a (hydro)peroxo-metal species, then, the O–O bond is cleaved heterolytically to form high-valent metal-oxo species as an active intermediate, which is responsible for the epoxidation of the uncoordinated cylehexene. If both reactants were coordinated, there would be plenty of time for further reactions. If cyclohexene was coordinated alone, the situation would not be much different from the stoichiometric reaction. Thus, probably, the role of the ligands is to exert steric influence on the accessibility of the central ion by the reactants.

## Conclusions

All the SOD-mimicking surface-anchored Fe(III)–amino acid complexes were successfully constructed. It was possible to prepare the covalently anchored complexes with uniform and mixed ligands as well. Covalent anchoring gave good control over the mode of immobilisation.

Analytical measurements revealed that mixtures of 1:1, 1:2 and 1:3 complexes were formed on the surface of the support. The coordination numbers and coordinating sites could be identified with the combination of XAS measurements, mid and far IR spectroscopies and chemical considerations. It was proven that the Fe(III) complexes were square pyramidal. The major coordinating sites were proposed to be the carboxylate oxygen, the imidazole nitrogen, the phenolate oxygen and sulphur atom of the thiolate group. The other coordination sites depended on the conditions of the synthesis and the structures of the molecules. In all cases water molecules saturated the coordination sphere. In most cases under ligand-excess conditions the surface-anchored ligand-poor complexes were rearranged.

All the covalently anchored complexes were active in a SOD test reaction: they could catalyse the dismutation reaction of the superoxide radical anion. The activity, in some cases, was only one magnitude lower that of the native Cu,ZnSOD enzyme.

The complexes displayed catalytic activity in the oxidation of cyclohexene, and all of them were extremely selective to cyclohexene oxide formation. There was no leaching of the ligands or the complex either during the reaction. Some of the best catalysts were reused twice without significant loss in the catalytic activity and selectivity. The activities were but the selectivities were basically not dependent on the coordinating groups.

Immobilisation of transition metal–amino acid complexes turned out to be a viable route for preparing efficient electron transfer catalysts, since there are very active and selective catalysts that can be easily recovered and recycled. They show the promise of becoming efficient catalysts in the synthesis of fine chemicals.

**Acknowledgments** This research was financed by the TÁMOP 4.2.2.A-11/1/KONV-2012-0047 and the OTKA 83889 grants. The supports are highly appreciated.

## References

1. K.M. Koeller, C.H. Wong, Nature **409**, 232 (2001)
2. U. Hanefeld, L. Gardossi, E. Magner, Chem.Soc.Rev. **38**, 453 (2009)
3. U.T. Bornscheuer, Angew. Chem. Int. Ed. **42**, 3336 (2003)
4. D.J. Xuereb, R. Raja, Catal. Sci. Technol. **1**, 517 (2011)
5. J.A. Labinger, J. Mol. Catal. A: Chem. **220**, 27 (2004)
6. M. Luechinger, A. Kienhöfer, G.D. Pirngruber, Chem. Mater. **18**, 1330 (2006)
7. K. Suzuki, P.D. Oldenburg, L. Que Jr., Angew. Chem., Int. Ed. **47**, 1887 (2008)
8. B.M. Weckhuysen, J. Am. Chem. Soc. **128**, 3208 (2006)
9. J.A. Tainer, E.D. Getzoff, J.S. Richardson, D.C. Richardson, Nature **306**, 284 (1983)
10. H.D. Youn, E.J. Kim, J.H. Roe, Y.C. Hah, S.O. Kang, Biochem. J. **318**, 889 (1996)
11. G.E.O. Borgstahl, H.E. Parge, M.J. Hickey, W.F. Beyer Jr., R.A. Hallewell, J.A. Tainer, Cell **71**, 107 (1992)
12. A.-F. Miller, in Handbook of Metalloproteins (A. Messerschmidt, R. Huber, K. Wieghardt, T. Poulos, eds.), Wiley, Chichester, 2001, pp. 668–682.
13. W.C. Stallings, K.A. Pattridge, R.K. Strong, M.L. Ludwig, J. Biol. Chem. **259**, 10695 (1984)
14. M.L. Ludwig, A.L. Metzger, K.A. Pattridge, W.C. Stallings, J. Mol. Biol. **219**, 335 (1991)
15. M.S. Lath, M.M. Dixon, K.A. Pattridge, W.C. Stallings, J.A. Fee, M.L. Ludwig, Biochem. **34**, 1646 (1995)
16. F. Farzaneh, S. Sohrabi, M. Ghiasi, M. Ghandi, V. Mehdi Ghandi, J. Porous Mater. **20**, 267 (2013)
17. M. Halma, K.A.D. de Freitas Castro, C. Taviot-Gueho, V. Prévot, C. Forano, F. Wypych, S. Nakagaki, J. Catal. **257**, 233 (2008)
18. A. Baso, L.D. Martin, C. Ebert, L. Gardossi, P. Linda, F. Sibilla, Tetrahedron Lett. 44, 5889 (2003)
19. H.H.P. Yiu, P.A. Wright, J. Mater. Chem. **15**, 3690 (2005)
20. C. Ispas, I. Sokolov, S. Andreescu, Anal. Bioanal. Chem. **393**, 543 (2009)
21. G.D. Pirngruber , L. Frunz, M. Lüchinger, Phys. Chem. Chem. Phys. **11**, 2928 (2009)
22. Y. Zhang, J. Zhao, L. He, D. Zhao, S. Zhang, Mic. Mes. Mater. **94**, 159 (2006)
23. J. Gao, Y. Chen, B. Han, Z. Feng, C. Li, N. Zhou, Z. Gao, J. Mol. Catal., A **210**, 197 (2004)
24. S. Samantaray, K. Parida, Catal. Commun. **6**, 578 (2005)
25. S. Bhattacharjee, J.A. Anderson, J. Mol. Catal. A **249**, 103 (2006)

26. J. Jiang , K. Ma, Y. Zheng, S. Cai, R. Li, J. Ma, Appl. Clay Sci. **45**, 117 (2009)
27. R. Noyori, M. Aoki, K. Sato, Chem. Commun. 1977 (2003)
28. T. Punniyamurthy, L. Rout, Coord. Chem. Rev. **252**, 134 (2008)
29. H. Shi, Z. Zhang, Y. Wang, J. Mol. Catal., A **238**, 13 (2005)
30. K.-P. Ho, W.-L. Wong, K.-M. Lam, C.-P. Lai, T.H. Chan, K.-Y. Wong, Chem. Eur. J. **14**, 7988 (2008)
31. A. Decker, E.I. Solomon, Curr. Opin. Chem. Biol. **9**, 152 (2005)
32. Z. Csendes, Cs. Dudás, G. Varga, É.G. Bajnóczi, S.E. Canton, P. Sipos, I. Pálinkó, J. Mol. Struct. **1044**, 39 (2013)
33. Z. Csendes, N. Földi, J.T. Kiss, P. Sipos, I.Pálinkó, J. Mol. Struct. **993**, 203 (2011)
34. S. Carlson, M. Clausen, L. Gridneva, B. Sommarin, C.J. Svensson, J. Synchrotron Radiat. **13**, 359 (2006)
35. B. Ravel, M. Newville, J. Synchrotron Radiat. **12**, 537 (2005)
36. J.J. Rehr, J.M. DeLeon, S.I. Zabinsky, R.C. Albers, J. Am. Chem. Soc. **113**, 5135 (1991)
37. S.K. Papageorgiou, E.P. Kouvelos, E.P. Favvas, A.A. Sapadilis, G.E. Romanos, F.K. Katsaros, Carbohydr. Res. **345**, 469 (2010)
38. S.A. Abdel-Latif, H.B. Hassib, Y.M. Issa, Spectrochim. Acta, Part A **67**, 950 (2007)
39. T. Miura, T. Satoh, H. Takeuchi, Biochim. Biophys. Acta **1384**, 171 (1998)
40. C. Beauchamp, I. Fridovich, Anal. Biochem. **44**, 276 (1971)
41. P. Chutia, S. Kato, T. Kojima, S. Satokawa, Polyhedron **28**, 370 (2009)
42. G. Bilis, K.C. Christoforidis, Y. Deligiannakis, M. Louloudi, Catal. Today **157**, 101 (2010)
43. S. Khare, R. Chokhare, J. Mol. Catal., A **344**, 83 (2011)